

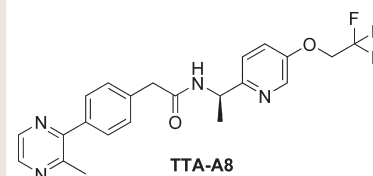
Short-Acting T-Type Calcium Channel Antagonists Significantly Modify Sleep Architecture in Rodents

Zhi-Qiang Yang,^{*,†} Kelly-Ann S. Schlegel,[†] Youheng Shu,[†] Thomas S. Reger,[†] Rowena Cube,[†] Christa Mattern,[†] Paul J. Coleman,[†] Jim Small,[†] George D. Hartman,[†] Jeanine Ballard,[†] Cuyue Tang,[†] Yuhsin Kuo,[†] Thomayant Prueksaritanont,[†] Cindy E. Nuss,[§] Scott Doran,[§] Steve V. Fox,[§] Susan L. Garson,[§] Yuxing Li,[§] Richard L. Kraus,[§] Victor N. Uebele,[§] Adekemi B. Taylor,[†] Wei Zeng,[†] Wei Fang,[†] Cynthia Chavez-Eng,[†] Matthew D. Troyer,^{||} Julie Ann Luk,^{||} Tine Laethem,^{||} William O. Cook,[⊥] John J. Renger,[§] and James C. Barrow[†]

Departments of [†]Medicinal Chemistry, [‡]Drug Metabolism and Pharmacokinetics, [§]Depression and Circadian Disorders, ^{||}Clinical Pharmacology, and [⊥]Toxicology Sciences, Merck Research Laboratories, WP14-3, P.O. Box 4, 770 Sumneytown Pike, West Point, Pennsylvania 19486

ABSTRACT A novel phenyl acetamide series of short-acting T-type calcium channel antagonists has been identified and evaluated using in vitro and in vivo assays. Heterocycle substitutions of the 4-position of the phenyl acetamides afforded potent and selective antagonists that exhibited desired short plasma half-lives across preclinical species. Lead compound TTA-A8 emerged as a compound with excellent in vivo efficacy as indicated by its significant modulation of rat sleep architecture in an EEG telemetry model, favorable pharmacokinetic properties, and excellent preclinical safety. TTA-A8 recently progressed into human clinical trials, and in line with our predictions, preliminary studies ($n = 12$) with a 20 mg oral dose afforded a high C_{\max} of $1.82 \pm 0.274 \mu\text{M}$ with an apparent terminal half-life of $3.0 \pm 1.1 \text{ h}$.

KEYWORDS Calcium channel antagonists, sleep, T-type calcium channels, electrocorticogram, pharmacokinetics



Voltage-gated calcium channels regulate the entry of Ca^{2+} into cells in response to membrane depolarization. The consequences of Ca^{2+} influx include further depolarization of the cell membrane, muscle contraction, neurotransmitter release, and many other events.¹ On the basis of cloning of the main pore-forming α -subunit, they can be divided into three main families: Cav1.x (L-type), Cav2.x (N-, P/Q-, R-type), and Cav3.x (T-type).² Recently, the T-type calcium channel has attracted a lot of interest for treatment of both peripheral and central nervous system (CNS) disorders.³ Of the three T-type calcium channels, the Cav3.1 and Cav3.3 subtypes are primarily expressed in the brain, while Cav3.2 has a broader central and peripheral expression.⁴ In the CNS, T-type calcium channels are highly expressed in the thalamus and cortex regions and play important roles in thalamocortical signaling.⁵ The corticothalamic loop consists of cortical pyramidal, thalamic relay, and reticular thalamic neurons whose resting membrane potential is modified by inputs from multiple neurotransmitter systems such as histamine, noradrenaline, and serotonin, resulting in control of the arousal state of the network. The resting membrane potential and the state of the T-type calcium channel determine one of two distinct network activities: tonic activity, which is associated with depolarization and the wake state, or bursting activity, which is associated

with hyperpolarization and slow-wave sleep (SWS).^{6,7} Thus, we sought to identify selective and brain-penetrant T-type channel blockers to evaluate how modulation of these channels could impact the thalamocortical network and vigilance state.

Our laboratories have previously disclosed two structurally distinct classes of T-type calcium channel antagonists: piperidines **1** and **2** and quinazolinone **3** (Figure 1).^{8–10} Both series showed good in vivo efficacy in epilepsy and tremor models while having minimal effects on cardiovascular parameters.^{8,9} Moreover, with both series, we observed significant effects on sleep architecture in rodent and rhesus electrocorticogram (ECoG) models.^{10,11} More recently, we disclosed another series of T-type antagonists exemplified by phenyl acetamide **4**.^{11,12,15} Similar to structurally distinct piperidines **1** and **2** and quinazolinone **3**, phenyl acetamide **4** exhibited robust effects on sleep architecture in rats, suggesting the common involvement of T-type calcium channels.

These promising results led us to focus on identifying compounds with shorter half-lives and good bioavailability,

Received Date: July 14, 2010

Accepted Date: August 18, 2010

Published on Web Date: August 24, 2010

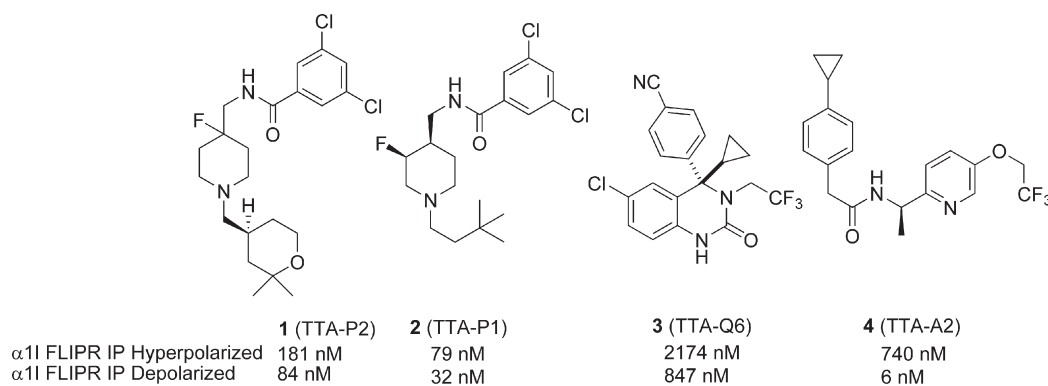
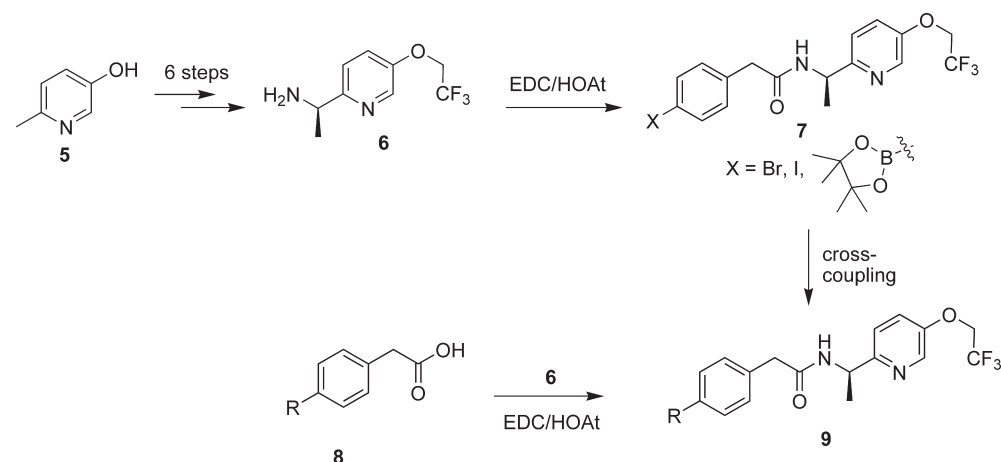


Figure 1. T-type calcium channel antagonists.

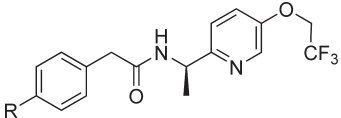
Scheme 1. General Synthetic Route to Heterocycle Amides **9**


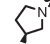

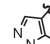
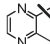


ideal for clinical evaluation as novel sleep agents. Here, we wish to report compounds from the phenyl acetamide class exhibiting desirable pharmacokinetic properties (Figure 1).

During the discovery of compound **4**,¹¹ it was noted that the trifluoroethoxypyridyl group is optimal for both potency and metabolic stability, whereas heterocycles are well tolerated as a replacement of the cyclopropyl group. In addition, heterocycle modifications generally provided compounds with improved physical properties and minimal or no pregnane X receptor (PXR) activity. Activation of PXR could lead to the induction of CYP3A enzymes and thus poses a potential risk of drug–drug interactions; therefore, minimization of this activity is desirable.¹⁵ To this end, we developed an efficient strategy to allow extensive screening of a wide array of heterocycles. The general synthetic route was illustrated in Scheme 1. Chiral amine **6** was synthesized from commercially available 3-hydroxyl picoline **5** in 31% over six steps with excellent stereoselectivity.¹² Amine **6** was coupled to either a 4-halo phenylacetic acid or 4-boronic ester phenylacetic acid to give intermediate **7**. Subsequent cross-coupling to install the heterocycles afforded compounds **9**. Alternatively, para-heterocycle-substituted phenyl acetic acid (general structure **8**) was constructed first and then coupled to amine **6** to afford the final amides **9**.

Potency on the T-type calcium channel was determined by a binding assay and two FLIPR assays designed to measure potency on the inactivated state of the channel (depolarized assay) and the resting state of the channel (hyperpolarized assay) as previously described.¹⁵ All compounds were also counter-screened against other ion channels, such as the human ether-a-go-go potassium channel (hERG)^{16,17} and L-type calcium channels.¹⁴ A group of representative examples containing diverse heterocycles are shown in Table 1, including saturated and aromatic heterocyclic rings. Comparing the two FLIPR assays, we noted a greater than 80-fold difference in potency depending on the resting membrane potential of the test cell line. Previously, we have shown that both state-independent piperidines **1** and **2** and state-dependent quinazolinones such as **3** were efficacious in our in vivo models, suggesting that binding to the inactivated state of the channel is sufficient for pharmacological effects. As a general trend, the phenyl acetamide class of compounds displayed excellent potency on T-type calcium channels and weak activity on hERG and L-type channels (IC_{50} values > 10 μ M). As shown in Table 1, compound **10** bearing a 3-fluoro pyrrolidine is extremely potent with an IC_{50} value of 4 nM in the depolarized FLIPR assay and a K_i value of 0.3 nM in the binding affinity assay.¹⁸ The 4-methyl oxazole-containing compound **11** and 3-substituted pyrazolo[1,5-b]pyridazine

Table 1. In Vitro and in Vivo Data for T-Type Calcium Channel Antagonists


R					
Compound #	4 (TTA-A2)	10 (TTA-A4)	11 (TTA-A5)	12 (TTA-A6)	13 (TTA-A8)
FLIPR depolarized (nM) ^a	9.4±4.4	3.7±1.4	5.3±1.9	5.4±1.9	31.3±10.9
FLIPR hyperpolarized (nM) ^a	384±266	249±86	206±140	397±197	1918±483
K _i (nM) ^b	1.2±0.3	0.3±0.1	0.2	NT	5.5±0.6
L-Type FLIPR (μM) ^c	>10	>10	>10	>10	>10
hERG (MK499 binding, μM) ^d	>10	>10	>30	>30	>30
WAG/Rij (% inhib. @ 4 h) ^e	87%	NT	72%	85%	87%
P-gp (B:A:A:B) ^f	0.7	1.1	1.1	1.3	1.3
Papp (10-6cm/s)	45	41	35	38	44
PXR (% Rif@ 10μM) ^g	17%	31%	7%	0%	8%
Dog iv CL _p (mL/min/kg) ^h	0.9	NT	5.7	16	9.0
Dog iv T _{1/2} (h)	11	NT	1.1	0.80	0.71
Dog iv V _{ss} (L/kg)	0.7	NT	0.36	0.54	0.45

^aData presented as the mean ± standard deviation as described in reference 15. ^bData presented as the mean ± standard deviation as described in reference 15 or the average of $n = 2$ measurements. ^cData are the average of $n = 2$ measurements. The assay is described in reference 14. ^dData are the average of $n = 2$ measurements. The assay is described in reference 17. ^eInhibition of seizure duration was calculated 4 h after 3 mpk oral dosing relative to vehicle dosing on the previous day as an average of $n = 2$ rats. ^fBasolateral to apical/apical to basolateral transport ratio in human MDR1 transfected cells (see reference 23). ^gPercent response of PXR activation relative to Rifampicin at 10 μM (see reference 27). ^hDog intravein cassettes in beagles, 0.125 mpk dose in DMSO ($n = 2$).

analogue **12** also exhibited excellent binding affinity and functional potency. A six-membered ring such as 2-methyl pyrazine derivative **13** showed good potency with an IC₅₀ value of 31 nM.

To be effective in inhibiting central T-type channels in vivo, compounds subjected to the efflux mediated by P-glycoprotein transporter (P-gp) should be avoided as this transporter can often limit brain penetration.²² Despite introducing additional hydrogen bond acceptors into general structure **9**, which might limit brain penetration,²³ compounds **10–13** showed low directional transport ratios (BA/AB < 2) in human P-gp expressing cell line and maintaining excellent cell permeability.²⁴ To rapidly evaluate compounds' ability to block central T-type channels, we employed a rat genetic model of absence epilepsy using Wistar Albino Glaxo rats bred in Rijswijk, The Netherlands (WAG/Rij), as reported previously.¹⁵ These rats display cortical EEG patterns and physical behaviors characteristic of absence epilepsy, including frequent seizures.²⁵ Because T-type calcium channels are involved in the regulation of thalamocortical rhythms that underlie these seizures, measurement of EEG in these animals serves as a relevant pharmacodynamic readout of brain penetration and T-type channel blockade. Consistent with our previous findings with compounds **1–4**, compounds **11–13** all displayed robust inhibition of time in seizure, with greater than 70% reduction over the first 4 h after oral dosing 3 mg/kg (Table 1).

Optimally, a compound designed to treat sleep disorders would be rapidly absorbed, readily crossing the blood–brain barrier and engaging the target at efficacious levels for the ~8 h duration of the sleep period. We preferred a compound with a restricted (predicted) human half-life. As the value of half-life is determined by systemic clearance (Cl) and

Table 2. Pharmacokinetic Parameters of **11**

species	CL _p (mL/min/kg)	T _{1/2} (h)	V _{ss} (L/kg)	F (%)	plasma PB (% bound) ^a
rat	35	0.4	1.1	100	5.2
dog	3.6	1.1	0.3	50	1.6

^aDetermined by ultracentrifugation with ¹⁴C-labeled **11** at 5 μM.

the volume of distribution at steady state (V_{ss}), T_{1/2} = 0.693 V_{ss}/Cl, a shorter half-life could be achieved via enhancing Cl or lowering V_{ss}. However, a high clearance compound is not desired due to the high propensity for drug–drug interactions.²⁶ Thus, another strategy is to strive for low to moderate clearance compounds with low V_{ss}. In the structural scaffolds that we have explored, the phenylacetamides generally showed these characteristics. To screen compounds for potential short half-lives in humans, we employed cassette intravenous administration to dogs as our primary pharmacokinetics screening tool to get a quick readout on clearance and V_{ss}. Among the compounds evaluated, compounds **11–13** appeared to possess the desired profile as their short half-lives were mainly attributed to their low V_{ss} (Table 1). On the basis of its potency and promising results from the initial pharmacokinetic screening, compound **11** was chosen for further single-dose pharmacokinetic profiling in preclinical species. As shown in Table 2, consistent with the finding from the dog intravenous cassette study, compound **11** displayed a T_{1/2} = 1.1 h in this species with a good bioavailability of 50%. In rats, compound **11** displayed a T_{1/2} = 24 min and was 100% bioavailable after dosing at 10 mg/kg.

However, further profiling of **11** revealed a high potential for bioactivation. Incubation of **11** in liver microsomes gave rise to a significant amount glutathione (GSH) adduct, which

was confirmed by NMR spectroscopy.²⁷ The formation of a covalent adduct was confirmed with a covalent labeling experiment.²⁸ Incubation of [¹⁴C]-labeled **11** (10 μ M) with human liver microsomes (1 mg/mL) for 60 min in the presence of NADPH yielded high levels of irreversible binding to microsomal proteins (1558 pmol equivalent/mg protein) (Table 3). Bioactivation was quickly addressed by replacing the oxazole ring with different heterocycles. For instance, fused bicyclic compound **12** showed a low amount of GSH adduct formation, which translated to a moderate level of covalently labeled human microsomal proteins (244 pmol equivalent/mg protein). Gratifyingly, no GSH adduct was detected with methylpyrazine derivative **13**. In agreement, incubation of [¹⁴C]-labeled **13** with human liver microsomes (1 mg/mL) yielded a minimal level of irreversible binding to microsomal proteins (< 10 pmol equivalent/mg protein), indicating a low potential of bioactivation. As a result, **13** was further characterized as a key compound of interest.

Table 3. Covalent Protein Binding of **11–13** in Human Microsome

compound	GSH adduct ^a	human in vitro covalent protein binding (pmol/mg protein) ^b
11	high	1558 \pm 109
12	low	244 \pm 28
13	no	8 \pm 1

^aAmount was semiquantified using LC-MS. ^bLabeled protein measured after incubation of [¹⁴C]-labeled **11–13** (10 μ M) with human liver microsomes (1 mg/mL) for 60 min in the presence of NADPH.

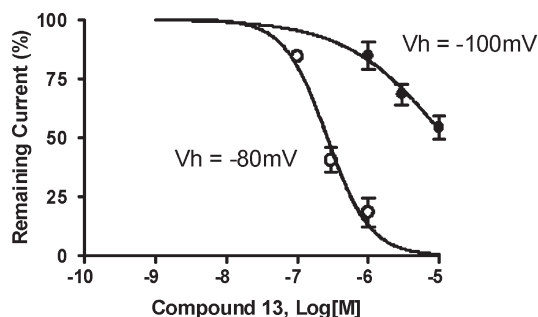


Figure 2. Inhibition of the T-type calcium channel Cav3.3 subtype by **13** as determined by standard voltage clamp. Data points reflect means \pm SEs of three determinations. The IC_{50} values of 264 nM and 12 μ M were determined at -80 and -100 mV, respectively.

Table 4. Pharmacokinetic Parameters of **13**

species	CL (predicted) ^a (mL/min/kg)	CL _p (observed) (mL/min/kg)	$T_{1/2}$ (h)	V_{ss} (L/kg)	F (%)	plasma PB (% unbound) ^b
rat	8	30.3	0.24	0.59	71	12.3
dog	13	11.8	0.81	0.36	23	15.5
rhesus	22	19.3	0.53	0.74	5	14.6
human	$\sim 1^c$		$< 5^c$	$< 0.4^c$		3.2

^aCL was predicted based on in vitro metabolic Cl_{int} with the well-stirred model. ^bDetermined by equilibrium dialysis with ¹⁴C-labeled **13** at 5 μ M. ^cPredicted human values.

The potency and state-dependent profile observed in the FLIPR assays were confirmed with whole cell patch clamp recording at two holding potentials, -100 and -80 mV. Compound **13** showed potencies of 12 μ M and 264 nM, respectively (Figure 2). To examine ion channel selectivity, compound **13** was assayed against important cardiac sodium and potassium channels using planar patch clamp technology. At the highest tested concentration of 30 μ M, compound **13** inhibited hERG current (I_{Kr}) by $41 \pm 4\%$ and had no effect on I_{Ks} . Likewise, at the highest tested concentration of 30 μ M, compound **13** had little effect on I_{Na} (20% inhibition at 3 Hz) and L-type I_{Ca} (12% at 30 μ M). In addition, the off-target activity of compound **13** was evaluated in a panel of 170 receptor binding or enzyme assays (MDS Pharma Services) and revealed no activities with IC_{50} values < 10 μ M.

To aid in the prediction of human pharmacokinetics, the pharmacokinetic profile of compound **13** was evaluated in three preclinical species, and data are shown in Table 4. It exhibits moderate to high plasma clearance (CL_p), low volume of distribution (V_{ss}), and a short half-life ($T_{1/2}$) in three preclinical species. In light of the greater extent of plasma protein binding of **13** in human than preclinical species (Table 4), the volume of distribution of **13** could be lower than the values observed in animals. The $T_{1/2}$ of **13** was predicted to be less than 5 h in humans.²⁹ As the distribution of **13** into human brain is not expected to be hampered by P-gp-mediated efflux, its free brain concentration may be reasonably reflected by its free plasma concentration. In preclinical settings, drug concentrations in the cerebrospinal fluid (CSF) have been widely used as the surrogate for free brain concentration. It was found that 30 min after oral dosing in rats, the concentration of **13** in the CSF and brain accounted for 4.3 and 38% of that in plasma, giving a free fraction in the brain of 11%, consistent with its free fraction in the plasma.

To evaluate the effects of T-type antagonists on sleep and wake, telemetric recordings of ECoG and electromyogram (EMG) signals were measured in rats. In a 7 day cross-over design, vehicle or compound **13** was dosed orally every day, 30 min before the inactive phase (lights on for rats). The ECoG and EMG signals were collected and scored for the amount of time awake or each phase of sleep (light sleep, delta sleep, and REM).

Remarkably, despite having a half-life of 14 min, a 5 mg/kg dose of **13** to rats prior to their inactive period produced a significant suppression of active wake for 1.5 h after dosing (Figure 3). In addition, a dose-dependent increase of delta

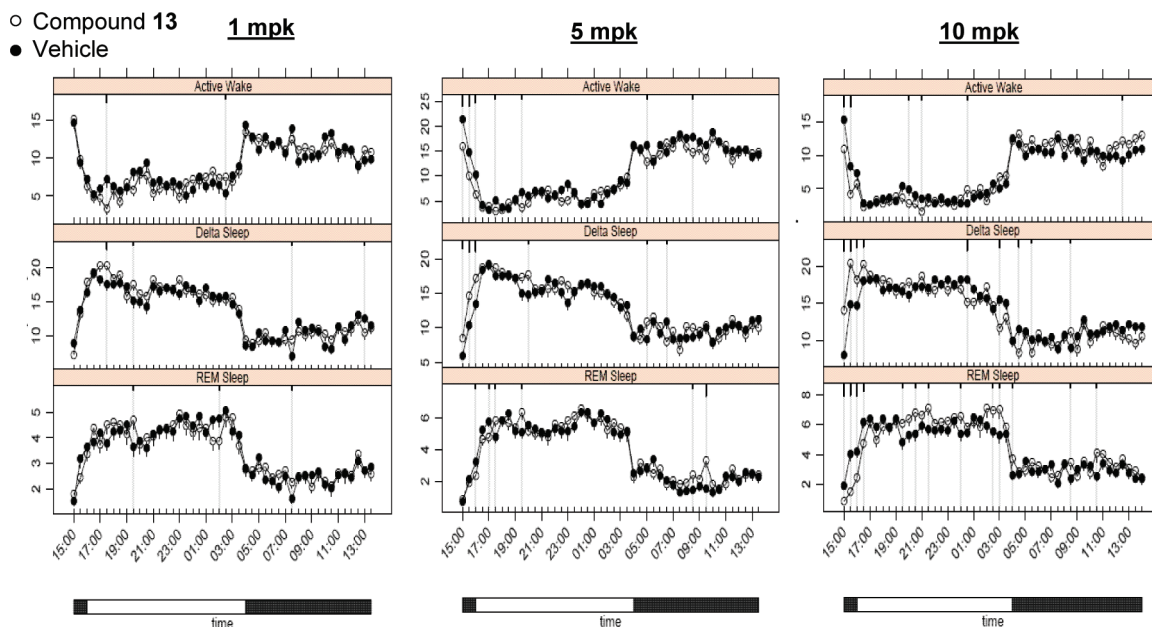


Figure 3. Effect of **13** on $N = 7$ male SD rat active sleep for 23 h after dosing 1, 5, and 10 mg/kg po. Data are average minutes of active wake, Delta sleep, and REM sleep in each 30 min bin (\pm SEM) starting at dose time (abscissa 15:00). The time bar below the x-axis denotes periods of lights on (\square , inactive phase) and lights off (\blacksquare , active phase). The significance at each time point is reported as tick marks (short $p < 0.05$, medium $p < 0.01$, and long $p < 0.001$) and gray vertical lines through significantly different comparisons based on a linear mixed effects ANOVA at each time point.

sleep was observed for 0.5–2.0 h after dose. Maximal plasma concentrations, as estimated from dosing nonimplanted satellite animals, were between 0.12 and 2.7 μM for doses ranging from 1 to 10 mg/kg at 0.1–0.7 h postdose.

On the basis of a favorable preclinical safety profile, desired PK properties, and good in vivo efficacy, compound **13** was advanced to human safety and tolerability studies. In line with our predictions, preliminary studies in human subjects ($n = 12$) with a 20 mg oral dose afforded a high C_{max} of $1.82 \pm 0.274 \mu\text{M}$ with an apparent terminal half-life of 3.0 ± 1.1 h.

In conclusion, replacement of the cyclopropane substituent of **4** with various heterocycles maintained potency and selectivity for the T-type calcium channel while modulating pharmacokinetics and resulted in the identification of the 2-methylpyrazine phenyl acetamide **13**. Compound **13** displayed excellent potency and selectivity for the T-type channel. It showed significant suppression of active wake and increased delta sleep in rats. Compound **13** progressed into human clinical trials and displayed a short half-life and good exposure as predicted. Phase I studies with a structurally related compound suggest that the qEEG effects may be species-dependent. The results will be disclosed in a separate account in due course.

SUPPORTING INFORMATION AVAILABLE Experimental procedures and analytical data for compounds **10–13**. This material is available free of charge via the Internet at <http://pubs.acs.org>.

AUTHOR INFORMATION

Corresponding Author: *To whom correspondence should be addressed. Tel: 215-652-2171. Fax: 215-652-3971. E-mail: zhiqiang_yang@merck.com.

ACKNOWLEDGMENT We thank Nicole Pudvah for P-gp measurements; Ken Anderson, Leslie Geer, and Debra McLoughlin for PK analysis; Charles Ross and Joan Murphy for high-resolution mass spectral analysis; Elena S. Trepakova for ion channel profiling; and Yuming Zhao, Joseph Simeone, and Eric Soli for ^{14}C -labeled compound synthesis.

REFERENCES

- (1) Zamponi, G. W. *Voltage-Gated Calcium Channels*; Kluwer Academic/Plenum Publishers: New York, 2005.
- (2) Ertel, E. A.; Campbell, K. P.; Harpold, M. M.; Hofmann, F.; Mori, Y.; Perez-Reyes, E.; Schwartz, A.; Snutch, T. P.; Tanabe, T.; Birnbaumer, L.; Tsien, R. W.; Catterall, W. A. Nomenclature of voltage-gated calcium channels. *Neuron* **2000**, *25*, 533–535.
- (3) Todorovic, S. M.; Jevtic-Todorovic, V. The Role of T-Type Calcium Channels in Peripheral and Central Pain Processing. *CNS Neurol. Disord.: Drug Targets* **2006**, *5*, 639–653.
- (4) Talley, E. M.; Cribbs, L. L.; Lee, J. H.; Daud, A.; Perez-Reyes, E.; Bayliss, D. A. Differential Distribution of Three Members of a Gene Family Encoding Low Voltage-Activated (T-Type) Calcium Channels. *J. Neurosci.* **1999**, *19*, 1895–1911.
- (5) Llinas, R. R.; Steriade, M. Bursting of thalamic neurons and states of vigilance. *J. Neurophysiol.* **2006**, *95*, 3297–3308.
- (6) Crunelli, V.; Cope, D. W.; Hughes, S. W. Thalamic T-type Ca^{2+} channels and NREM sleep. *Cell Calcium* **2006**, *40*, 175–190.
- (7) Cueni, L.; Canepari, M.; Adelman, J. P.; Luthi, A. Ca^{2+} signaling by T-type Ca^{2+} channels in neurons. *Pflugers Arch. Eur. J. Physiol.* **2009**, *457*, 1161–1172.
- (8) Shipe, W. D.; Barrow, J. C.; Yang, Z. Q.; Lindsley, C. W.; Yang, F. V.; Schlegel, K. A. S.; Shu, Y.; Rittle, K. E.; Bock, M. G.; Hartman, G. D.; Tang, C.; Ballard, J. E.; Kuo, Y.; Adarayan, E. D.; Prueksaritanont, T.; Zrada, M. M.; Uebele, V. N.; Nuss, C. E.; Connolly, T. M.; Doran, S. M.; Fox, S. V.; Kraus, R. L.;

- Marino, M. J.; Gratfelds, V. K.; Vargas, H. M.; Bunting, P. B.; Hasbun-Manning, M.; Evans, R. M.; Koblan, K. S.; Renger, J. J. Design, synthesis, and evaluation of a novel 4-aminomethyl-4-fluoropiperidine as a T-type Ca²⁺ channel antagonist. *J. Med. Chem.* **2008**, *51*, 3692–3695.
- (9) Yang, Z. Q.; Barrow, J. C.; Shipe, W. D.; Schlegel, K. A. S.; Shu, Y. S.; Yang, F. V.; Lindsley, C. W.; Rittle, K. E.; Bock, M. G.; Hartman, G. D.; Uebele, V. N.; Nuss, C. E.; Fox, S. V.; Kraus, R. L.; Doran, S. M.; Connolly, T. M.; Tang, C. Y.; Ballard, J. E.; Kuo, Y. S.; Adarayan, E. D.; Prueksaritanont, T.; Zrada, M. M.; Marino, M. J.; Graufelds, V. K.; DiLella, A. G.; Reynolds, I. J.; Vargas, H. M.; Bunting, P. B.; Woltmann, R. F.; Magee, M. M.; Koblan, K. S.; Renger, J. J. Discovery of 1,4-Substituted Piperidines as Potent and Selective Inhibitors of T-Type Calcium Channels. *J. Med. Chem.* **2008**, *51*, 6471–6477.
- (10) Barrow, J. C.; Rittle, K. E.; Reger, T. S.; Yang, Z. Q.; Boniskey, P.; McGaughey, G.; Bock, M. G.; Hartman, G. D.; Tang, C. Y.; Ballard, J. E.; Kuo, Y. S.; Prueksaritanont, T.; Nuss, C. E.; Doran, S. M.; Fox, S. V.; Garson, S.; Kraus, R. L.; Li, Y.; Marino, M. J.; Graufelds, V. K.; Uebele, V. N.; Renger, J. J. Discovery of 4,4-Disubstituted Quinazolin-2-ones as T-Type Calcium Channels Antagonists. *ACS Med. Chem. Lett.* **2010**, *1*, 75–79.
- (11) Doran, S. Manuscript in preparation.
- (12) Reger, T. S. Manuscript in preparation.
- (13) Gao, Y. D.; Olson, S. H.; Balkovec, J. M.; Zhu, Y.; Royo, I.; Yabut, J.; Evers, R.; Tan, E. Y.; Tang, W.; Hartley, D. P.; Mosley, R. T. Attenuating pregnane X receptor (PXR) activation: A molecular modelling approach. *Xenobiotica* **2007**, *37*, 124–138.
- (14) Xia, M. H.; Imredy, J. P.; Koblan, K. S.; Bennett, P.; Connolly, T. M. State-dependent inhibition of L-type calcium channels: Cell-based assay in high-throughput format. *Anal. Biochem.* **2004**, *327*, 74–81.
- (15) Uebele, V. N.; Nuss, C. E.; Fox, S. V.; Garson, S. L.; Cristescu, R.; Doran, S. M.; Kraus, R. L.; Santarelli, V. P.; Li, Y.; Barrow, J. C.; Yang, Z. Q.; Schlegel, K. A.; Rittle, K. E.; Reger, T. S.; Bednar, R. A.; Lemaire, W.; Mullen, F. A.; Ballard, J. E.; Tang, C.; Dai, G.; McManus, O. B.; Koblan, K. S.; Renger, J. J. Positive allosteric interaction of structurally diverse T-type calcium channel antagonists. *Cell Biochem. Biophys.* **2009**, *55*, 81–93.
- (16) Raab, C. E.; Butcher, J. W.; Connolly, T. M.; Karczewski, J.; Yu, N. X.; Staskiewicz, S. J.; Liverton, N.; Dean, D. C.; Melillo, D. G. Synthesis of the first sulfur-35-labeled hERG radioligand. *Bioorg. Med. Chem. Lett.* **2006**, *16*, 1692–1695.
- (17) Butcher, J. W.; Claremon, D. A.; Connolly, T. M.; Dean, D. C.; Karczewski, J.; Koblan, K. S.; Kostura, M. J.; Liverton, N. J.; Melillo, D. G. Radioligand and binding assay. PCT Int. Appl. WO 2002005860, 2002.
- (18) The somewhat basic pyrrolidine of compound **10** imparts a modest LogP of 3.0 without engendering P-gp susceptibility, and these properties make it attractive as a potential ¹⁸F-labeled ligand for positron emission tomography (PET) (see references 19, 20, and 21).
- (19) Eckelman, W. C.; Gibson, R. E.; Rzeszotarski, W. J.; Vieras, F.; Mazaitis, J. K.; Francis, B.; Reba, W. C. The design of receptor binding radiotracers. In *Principles of Radiopharmacology*; Colombetti, L., Ed.; CRC Press: New York, 1979; pp 251–274.
- (20) Waterhouse, R. N. Determination of lipophilicity and its use as a predictor of blood-brain barrier penetration of molecular imaging agents. *Mol. Imaging Biol.* **2003**, *5*, 376–389.
- (21) Sanabria-Bohorquez, S.; Li, W.; Eng, W.; Ryan, C.; Riffel, K.; Zeng, Z.; Uebele, V.; Reger, T.; Barrow, J.; Williams, D., Jr.; Voll, R. J.; Howell, L.; Votaw, J.; Goodman, M. M.; Hamill, T. G. Evaluation of the alpha 1i T-type calcium channel PET tracer [¹⁸F]TTA-A4 in an anesthetized or conscious monkey. *J. Labelled Compd. Radiopharm.* **2009**, *52*, 402–402.
- (22) Doan, K. M. M.; Humphreys, J. E.; Webster, L. O.; Wring, S. A.; Shampine, L. J.; Serabjit-Singh, C. J.; Adkison, K. K.; Polli, J. W. Passive permeability and P-glycoprotein-mediated efflux differentiate central nervous system (CNS) and non-CNS marketed drugs. *J. Pharmacol. Exp. Ther.* **2002**, *303*, 1029–1037.
- (23) Friden, M.; Winiwarter, S.; Jerndal, G.; Bengtsson, O.; Wan, H.; Bredberg, U.; Hammarlund-Udenaes, M.; Antonsson, M. Structure-Brain Exposure Relationships in Rat and Human Using a Novel Data Set of Unbound Drug Concentrations in Brain Interstitial and Cerebrospinal Fluids. *J. Med. Chem.* **2009**, *52*, 6233–6243.
- (24) Hochman, J. H.; Pudvah, N.; Qiu, J.; Yamazaki, M.; Tang, C.; Lin, J. H.; Prueksaritanont, T. Interactions of human P-glycoprotein with simvastatin, simvastatin acid, and atorvastatin. *Pharm. Res.* **2004**, *21*, 1686–1691.
- (25) Coenen, A. M. L.; Drinkenburg, W. H. I. M.; Inoue, M.; Vanluijtelaaar, E. L. J. M. Genetic Models of Absence Epilepsy, with Emphasis on the Wag Rij Strain of Rats. *Epilepsy Res.* **1992**, *12*, 75–86.
- (26) Lin, J. H.; Lu, A. Y. H. Interindividual variability in inhibition and induction of cytochrome P40 enzymes. *Annu. Rev. Pharmacol. Toxicol.* **2001**, *41*, 535–67.
- (27) See the Supporting Information.
- (28) Tang, C.; Subramanian, R.; Kuo, Y.; Krymgold, S.; Lu, P.; Kuduk, S. D.; Ng, C.; Feng, D. M.; Elmore, C.; Soli, E.; Ho, J.; Bock, M. G.; Baillie, T. A.; Prueksaritanont, T. Bioactivation of 2,3-diaminopyridine-containing bradykinin B-1 receptor antagonists: Irreversible binding to liver microsomal proteins and formation of glutathione conjugates. *Chem. Res. Toxicol.* **2005**, *18*, 934–945.
- (29) A good in vivo–in vitro correlation of clearance was observed in the dog and rhesus monkey but not in the rat. The high bioavailability (71 %) in contrast to the relatively high clearance in the rat may suggest the contribution of extrahepatic clearance in this species. Therefore, prediction of human clearance was performed based on the dog and monkey data, which resulted in an approximated value of 1 mL/min/kg. On the basis of the estimated values of volume of distribution (<0.4 L/kg based on unbound V_{ss} scaling) and clearance, the half-life of **13** was predicted to be less than 5 h in humans.